Thermochimica Acta, 207 (1992) 85–93
Elsevier Science Publishers B.V., Amsterdam

Thermal and calorimetric investigations of $M(IO_3)_2 \cdot H_2O$ and $M(IO_3)_2 \cdot D_2O$ ($M^{2+} = Ca^{2+}$, Sr^{2+}, Ba^{2+})

M. Maneva and V. Koleva

Department of Inorganic Chemistry, Technological University, Sofia (Bulgaria)

(Received 10 February 1992)

Abstract

Thermal and calorimetric investigations were carried out on $M(IO_3)_2 \cdot H_2O$ and $M(IO_3)_2 \cdot D_2O$ ($M^{2+} = Ca^{2+}$, Sr^{2+}, Ba^{2+}) using DTA and DSC. We investigate the thermal behaviour of the ordinary and deuterated monohydrates, and discuss the differences observed between them. The enthalpy of the dehydration processes is determined. The $\Delta H^{\ominus}_{deh}$ data were used to calculate the value of $\Delta H_f^{\ominus}$ for the investigated monohydrates and monodeuterates. Comments are presented in relation to the isotope effect with regard to $\Delta H^{\ominus}_{deh}$ and $T_{max,deh}$.

INTRODUCTION

The thermal dehydration of $Ca(IO_3)_2 \cdot H_2O$ has been investigated by the TG and DTA methods in refs. 1–6, of $Sr(IO_3)_2 \cdot H_2O$ in refs. 5–8 and of $Ba(IO_3)_2 \cdot H_2O$ in refs. 1, 5, 6 and 9. Fuller and more detailed data on the thermal dehydration of all three alkaline-earth iodate hydrates are contained in ref. 5, the DTA curves being used to determine the E^* and $\Delta H^{\ominus}$ of dehydration. Data obtained calorimetrically about the $\Delta H^{\ominus}_{deh}$ for the investigated monohydrates are contained in ref. 10. According to refs. 1–3, 5, 7 and 11, the anhydrous salts obtained by thermal dehydration undergo decomposition by Ramelsberg's reaction, i.e. to orthoperiodate, iodine and oxygen. The activation energy and the order of the decomposition reactions are determined in ref. 11. DSC curves of $M(IO_3)_2 \cdot H_2O$ ($M^{2+} = Ca^{2+}$, Sr^{2+}, Ba^{2+}) which show effects attributed to polymorphic transformations in the case of the anhydrous salts have been obtained in the most recent investigations [12]. For $Ba(IO_3)_2$ such data have also been reported previously [11]. The existence of polymorphic transformations has been confirmed [12,13] through high-temperature Raman and X-ray inves-

Correspondence to: M. Maneva, Department of Inorganic Chemistry, Technological University, Sofia, Bulgaria.

tigations of the initial compounds, and through the IR spectra of the polymorphic forms.

In the light of the literature data, it was of interest to take the DTA, TG and DSC curves of $M(IO_3)_2 \cdot H_2O$ at a lower heating rate and to compare them with those of $M(IO_3)_2 \cdot D_2O$. No data whatever have been published for the deuterates, and this accounts for the interest shown in their investigation. The data obtained about the ordinary and deuterated hydrates provide information about the character of the isotope effect in the investigated compounds. This was the aim of our present investigation.

EXPERIMENTAL

The monohydrates investigated were obtained by precipitation from 30% solutions of the respective nitrates with iodic acid at 40–50°C to obtain $Ca(IO_3)_2 \cdot H_2O$ and at room temperature for $Sr(IO_3)_2 \cdot H_2O$ and $Ba(IO_3)_2 \cdot H_2O$. The deuterated derivatives were synthesized in an analogous manner by using 30% solutions of anhydrous nitrates and HIO_3 in heavy water. The process of sedimentation of the ordinary and deuterated hydrates was carried out under strictly identical conditions which guarantee particles of equal size. The crystalline phases sedimented were filtered and then dried in a flow of argon, and were kept in an inert medium. The reagents used were p.a. grade; D_2O was 99.75% (p.a. Merck). The monohydrates obtained were identified by quantitative analysis: Ca^{2+}, Sr^{2+} and Ba^{2+} complexometrically [14], iodine iodometrically [15], and water thermogravimetrically. The thermal investigations were carried out on derivatograph Paulik–Paulik–Erdey MOM OD-102 at heating rate (v) 5°C min^{-1} and sample weight 200 mg. DSC was undertaken on a Perkin-Elmer DSC-4 from 50 to 250°C; sample mass 1 mg in volatile sample pans. The enthalpies of the phase transitions were determined with $\pm 0.5\%$ accuracy, and the corresponding temperatures to ± 0.1°C. The diffractograms of the investigated compounds show that the pairs of ordinary–deuterated hydrates are crystallographically identical. The anhydrous salts obtained after thermal dehydration were identified by IR and X-ray methods.

EXPERIMENTAL RESULTS AND DISCUSSION

The DTA and TG curves of the three pairs of hydrates are presented in Fig. 1 for $Ca(IO_3)_2 \cdot H_2O$ (D_2O), in Fig. 2 for $Sr(IO_3)_2 \cdot H_2O$ (D_2O), and in Fig. 3 for $Ba(IO_3)_2 \cdot H_2O$ (D_2O). The DSC curves for $M(IO_3)_2 \cdot H_2O$ (D_2O) are shown in Fig. 4. Table 1 shows the results for thermal dehydration of the investigated compounds from the DTA and TG curves, and Table 2 shows those from DSC.

It follows from an analysis of the DTA and TG curves presented (Figs. 1–3) that the dehydration process in $Sr(IO_3)_2 \cdot H_2O$ and $Ba(IO_3)_2 \cdot H_2O$

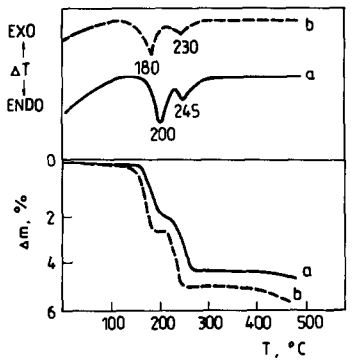

Fig. 1. DTA and TG curves of $Ca(IO_3)_2 \cdot H_2O$ (curves a) and $Ca(IO_3)_2 \cdot D_2O$ (curves b).

and in their deuterated analogues takes place in one stage, analogous to the data in the literature, until the corresponding anhydrous salts are obtained (Table 1). In the case of $Ca(IO_3)_2 \cdot H_2O$ and $Ca(IO_3)_2 \cdot D_2O$, however, the derivatograms each show two endoeffects corresponding to a decrease of the sample mass along the TG curve. This shows a two-stage course of the dehydration process, which has been observed for the first time by us.

The anhydrous salts obtained by thermal dehydration were identified mainly through their IR spectra, because no X-ray data exist concerning most of their polymorphic forms. The IR spectra taken were compared with those presented in refs. 12 and 13 relating to all familiar polymorphic modifications of the alkaline earth iodates.

It was established that the dehydration of $Ca(IO_3)_2 \cdot H_2O$ and $Ca(IO_3)_2 \cdot D_2O$ yields β-$Ca(IO_3)_2$ which undergoes no change until its decomposition (Table 1). $Ba(IO_3)_2 \cdot H_2O$ and its deuterated analogue yield the low-temperature α-form of the anhydrous salt which at $T_{max} = 390°C$ (375°C for the deuterate) undergoes polymorphic transformation into the high-

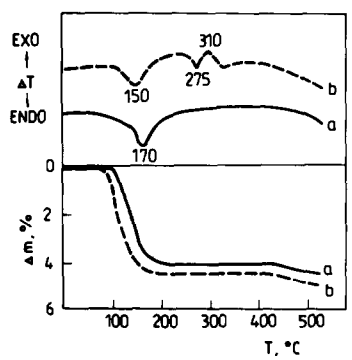

Fig. 2. DTA and TG curves of $Sr(IO_3)_2 \cdot H_2O$ (curves a) and $Sr(IO_3)_2 \cdot D_2O$ (curves b).

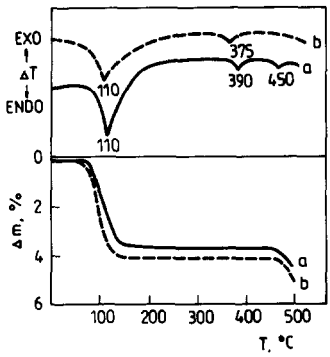

Fig. 3. DTA and TG curves of $Ba(IO_3)_2 \cdot H_2O$ (curves a) and $Ba(IO_3)_2 \cdot D_2O$ (curves b).

temperature β-form. The samples isolated at 420°C have an IR spectrum identical to that from ref. 12 for β-$Ba(IO_3)_2$. The existence of this is proved in ref. 12 by analysis of the data from the high-temperature (from 25 to 470°C) X-ray and Raman investigations. The temperature of polymorphic transformation has also been determined as 400 and 405°C respectively [12]. Recorded in the DTA curve of $Ba(IO_3)_2 \cdot H_2O$ (Fig. 3, curves a) is yet another small endoeffect at $T_{max} = 450$°C, which does not correspond to the change in the TG curve. Bearing in mind the data obtained in ref. 9, this endoeffect could be attributed to one more polymorphic transformation, namely β-$Ba(IO_3)_2 \rightarrow \gamma$-$Ba(IO_3)_2$. However, we do not have proof for such an explanation.

The DTA and TG curves of $Sr(IO_3)_2 \cdot H_2O$ and of its deuterated analogue are also interesting (Fig. 2, Table 1) because they reveal essential differences. For instance, the DTA curve of the ordinary hydrate shows only one endoeffect corresponding to the dehydration process forming β-$Sr(IO_3)_2$. The latter has been identified through its IR spectrum. How-

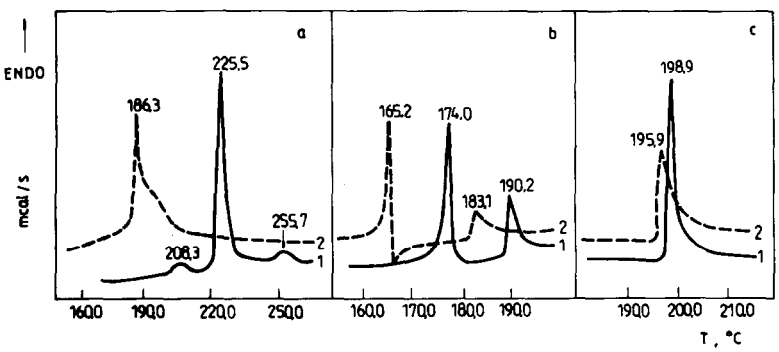

Fig. 4. DSC curves of (a) $Ca(IO_3)_2 \cdot H_2O$ (curve 1) and $Ca(IO_3)_2 \cdot D_2O$ (curve 2); (b) $Sr(IO_3)_2 \cdot H_2O$ (curve 1) and $Sr(IO_3)_2 \cdot D_2O$ (curve 2); (c) $Ba(IO_3)_2 \cdot H_2O$ (curve 1) and $Ba(IO_3)_2 \cdot D_2O$ (curve 2).

TABLE 1

DTA and TG data for $M(IO_3)_2 \cdot H_2O$ and $M(IO_3)_2 \cdot D_2O$ ($M^{2+} = Ca^{2+}$, Sr^{2+}, Ba^{2+})

Compound	Phase transition	Δm (%)		T_{max} (°C)	T_{init} (°C)
		Exp.	Theor.		
$Ca(IO_3)_2 \cdot H_2O$	$Ca(IO_3)_2 \cdot H_2O \rightarrow Ca(IO_3)_2 \cdot \frac{1}{2}H_2O + \frac{1}{2}H_2O$	2.2	2.2	200	–
	$Ca(IO_3)_2 \cdot \frac{1}{2}H_2O \rightarrow \beta\text{-}Ca(IO_3)_2 + \frac{1}{2}H_2O$	2.3	2.2	245	–
	$\beta\text{-}Ca(IO_3)_2 \rightarrow \frac{1}{5}Ca_5(IO_5)_2 + \frac{4}{5}I_2 + \frac{9}{5}O_2$	–	–	–	400
$Ca(IO_3)_2 \cdot D_2O$	$Ca(IO_3)_2 \cdot D_2O \rightarrow Ca(IO_3)_2 \cdot \frac{1}{2}D_2O + \frac{1}{2}D_2O$	2.5	2.43	180	–
	$Ca(IO_3)_2 \cdot \frac{1}{2}D_2O \rightarrow \beta\text{-}Ca(IO_3)_2 + \frac{1}{2}D_2O$	2.5	2.43	230	–
	$\beta\text{-}Ca(IO_3)_2 \rightarrow \frac{1}{5}Ca_5(IO_5)_2 + \frac{4}{5}I_2 + \frac{9}{5}O_2$	–	–	–	380
$Sr(IO_3)_2 \cdot H_2O$	$Sr(IO_3)_2 \cdot H_2O \rightarrow \beta\text{-}Sr(IO_3)_2 + H_2O$	4.2	3.95	170	–
	$\beta\text{-}Sr(IO_3)_2 \rightarrow \frac{1}{5}Sr_5(IO_5)_2 + \frac{4}{5}I_2 + \frac{9}{5}O_2$	–	–	–	420
$Sr(IO_3)_2 \cdot D_2O$	$Sr(IO_3)_2 \cdot D_2O \rightarrow \alpha\text{-}Sr(IO_3)_2 + D_2O$	4.1	4.3	150	–
	$\alpha\text{-}Sr(IO_3)_2 \rightarrow \gamma\text{-}Sr(IO_3)_2$	–	–	275	–
	$\gamma\text{-}Sr(IO_3)_2 \rightarrow \beta\text{-}Sr(IO_3)_2$	–	–	310	–
	$\beta\text{-}Sr(IO_3)_2 \rightarrow \frac{1}{5}Sr_5(IO_5)_2 + \frac{4}{5}I_2 + \frac{9}{5}O_2$	–	–	–	405
$Ba(IO_3)_2 \cdot H_2O$	$Ba(IO_3)_2 \cdot H_2O \rightarrow \alpha\text{-}Ba(IO_3)_2 + H_2O$	3.5	3.56	110	–
	$\alpha\text{-}Ba(IO_3)_2 \rightarrow \beta\text{-}Ba(IO_3)_2$	–	–	390	–
	$\beta\text{-}Ba(IO_3)_2 \rightarrow \frac{1}{5}Ba_5(IO_5)_2 + \frac{4}{5}I_2 + \frac{9}{5}O_2$	–	–	–	460
$Ba(IO_3)_2 \cdot D_2O$	$Ba(IO_3)_2 \cdot D_2O \rightarrow \alpha\text{-}Ba(IO_3)_2 + D_2O$	4.1	3.94	110	–
	$\alpha\text{-}Ba(IO_3)_2 \rightarrow \beta\text{-}Ba(IO_3)_2$	–	–	375	–
	$\beta\text{-}Ba(IO_3)_2 \rightarrow \frac{1}{5}Ba_5(IO_5)_2 + \frac{4}{5}I_2 + \frac{9}{5}O_2$	–	–	–	460

ever, the DTA curve of the deuterate shows one more endoeffect at $T_{max} = 275°C$, followed immediately by an exoeffect at $T_{max} = 310°C$, with the TG curve showing no change. Because the sample isolated immediately after dehydration ($\approx 220°C$) corresponds to $\alpha\text{-}Sr(IO_3)_2$, whereas that isolated at 400°C corresponds to $\beta\text{-}Sr(IO_3)_2$, the effects recorded can be explained by the polymorphic transformations (Table 1)

at $T = 275°C$ $\quad \alpha\text{-}Sr(IO_3)_2 \rightarrow \gamma\text{-}Sr(IO_3)_2$ $\quad$ endoeffect

at $T = 310°C$ $\quad \gamma\text{-}Sr(IO_3)_2 \rightarrow \beta\text{-}Sr(IO_3)_2$ $\quad$ exoeffect

However, owing to the immediate proximity of the two effects in the investigated derivatograms, the γ-form was not isolated and its involvement was not proved. Nevertheless, the proposed explanation of these effects is confirmed by high-temperature X-ray and Raman investigations of $Sr(IO_3)_2 \cdot H_2O$ [13]. The same effects were also recorded in the DSC curve of $Sr(IO_3)_2 \cdot H_2O$ at $v = 5°C\ min^{-1}$, but not in the DSC curve at $v = 10°C\ min^{-1}$, nor in the DTA curve [12]. During our investigations these polymorphic transformations were manifest in the DTA curve of the deuterate

TABLE 2

DSC data for $M(IO_3)_2 \cdot H_2O$ and $M(IO_3)_2 \cdot D_2O$ ($M^{2+} = Ca^{2+}$, Sr^{2+}, Ba^{2+})

Compound	Phase transition	$T_{ph.t.}$ (°C)		$\Delta H^{\ominus}_{ph.t.}$ (kJ mol^{-1})		$\Delta H^{\ominus}_{deh}$ (kJ mol^{-1})	
		T_{onset}	T_{max}	From DSC	From ref. 10	$\Delta H_f^{\ominus}$ $(H_2O)(g)$	$\Delta H_f^{\ominus}$ $(H_2O)(l)$
$Ca(IO_3)_2 \cdot H_2O$	$Ca(IO_3)_2 \cdot H_2O(s) \rightarrow \alpha\text{-}Ca(IO_3)_2(s) + H_2O(l)$	203.1	208.3	4.9	49.2	49.2	5.0
	$H_2O(l) \rightarrow H_2O(g)$	224.0	225.5	43.9			
	$\alpha\text{-}Ca(IO_3)_2(s) \rightarrow \beta\text{-}Ca(IO_3)_2(s)$	249.0	255.7	4.9	–	–	–
$Ca(IO_3)_2 \cdot D_2O$	$Ca(IO_3)_2 \cdot D_2O(s) \rightarrow Ca(IO_3)_2(s) + D_2O(g)$	185.1	186.3	56.6	–	59.9	14.5
$Sr(IO_3)_2 \cdot H_2O$	$Sr(IO_3)_2 \cdot H_2O(s) \rightarrow Sr(IO_3)_2(s) + H_2O(g)$	172.5	174.0	30.2	47.2	49.3	0.2
		188.5	190.2	15.8			
$Sr(IO_3)_2 \cdot D_2O$	$Sr(IO_3)_2 \cdot D_2O(s) \rightarrow Sr(IO_3)_2(s) + D_2O(g)$	163.6	165.2	37.2	–	59.9	1.5
		180.9	183.1	12.2			
$Ba(IO_3)_2 \cdot H_2O$	$Ba(IO_3)_2 \cdot H_2O(s) \rightarrow Ba(IO_3)_2(s) + H_2O(g)$	197.6	198.9	40.5	48.9	50.9	6.9
$Ba(IO_3)_2 \cdot D_2O$	$Ba(IO_3)_2 \cdot D_2O(s) \rightarrow Ba(IO_3)_2(s) + D_2O(g)$	194.6	195.9	38.7	–	59.9	14.5

alone, probably because they are energetically more significant in it, which is favourable for their detection. The examined effects lie in a temperature region outside that investigated by us through DSC.

The decomposition of the anhydrous salts obtained to the corresponding orthoperiodates, iodine and oxygen begins at temperatures above 400°C, according to refs. 1–3, 5 and 7.

The DTA data obtained for $M(IO_3)_2 \cdot H_2O$ ($M^{2+} = Ca^{2+}$, Sr^{2+}, Ba^{2+}) confirm the order established in ref. 5 for the thermal stability of the investigated monohydrates, which decreases from $Ca(IO_3)_2 \cdot H_2O$ to $Ba(IO_3)_2 \cdot H_2O$. There is a similar increase of the thermal stability of the anhydrous salts. These trends are also observed for the deuterated analogues. However, a comparison of the thermal stability of each pair of ordinary–deuterated hydrates shows that $M(IO_3)_2 \cdot D_2O$ ($M^{2+} = Ca^{2+}$, Sr^{2+}) have T_{max} of dehydration 20°C lower than that in $M(IO_3)_2 \cdot H_2O$ ($M^{2+} = Ca^{2+}$, Sr^{2+}). No such difference is recorded for $Ba(IO_3)_2 \cdot D_2O$ and $Ba(IO_3)_2 \cdot H_2O$, but it may be assumed that it is insignificant and is within the range of the error of the DTA method. We have also observed a large isotope effect ($T_{max} \approx 15$–20°C) in the ordinary and deuterated iodate hexahydrates of calcium and strontium [16].

The data obtained from the DSC curves (Fig. 4) make it possible to determine the enthalpies of the phase transitions taking place, particularly that of the dehydration process $\Delta H^{\ominus}_{deh}$. A comparison of this with those calculated according to Hess's law (Table 2) shows that the hydrate water released passes entirely into a gaseous state. For $Ca(IO_3)_2 \cdot H_2O$ the DSC curve (Fig. 4(a), curve 1) makes it possible to distinguish clearly between the two stages of the dehydration process, namely the release of the water ($\Delta H^{\ominus}_{diss}$) and the evaporation of the hydrate water released ($\Delta H^{\ominus}_{vap}$). Moreover, the values recorded for the enthalpies are in good agreement with those calculated (Table 2). It is demonstrated that $\Delta H^{\ominus}_{diss} = 4.9$ kJ mol^{-1}, and $\Delta H^{\ominus}_{vap} = 43.9$ kJ mol^{-1}. The latter value is higher than the one given in the literature for $\Delta H^{\ominus}_{vap}$ of pure water at the relevant temperature [17], and this higher value can be explained by the solubility of the anhydrous salt obtained in the hydrate water released. The slight endoeffect with $T_{max} = 255.7$°C may be attributed to polymorphic transformation of α- into β-$Ca(IO_3)_2$ as described by us for $Ca(IO_3)_2 \cdot 6H_2O$ (D_2O) [16]. Note that in the DSC curve of the deuterate (Fig. 4(a), curve 2) the above-mentioned distinction of the release of the water from its subsequent evaporation is only just perceptible, the first endoeffect passing into the second one. The expansion observed in the right part of the endoeffect shows the course of an additional phase transition which cannot be proved.

Two endoeffects may be observed in each of the DSC curves of $Sr(IO_3)_2 \cdot H_2O$ and $Sr(IO_3)_2 \cdot D_2O$ (Fig. 4(b)). They can be explained by two-stage dehydration, without corresponding to a particular stoichiometric transition. This assumption is based on the following: firstly, there is evidence [8]

that the same effect has been observed in the derivatogram of $Sr(IO_3)_2 \cdot H_2O$ (though we do not find it along the DTA curve (Fig. 2)), and secondly, the summed enthalpy ($\Delta H^{\ominus} = 46.0$ kJ mol^{-1}) of the two endoeffects is in good agreement with the calculations according to Hess's law (Table 2) and with the value determined calorimetrically in ref. 10.

The sole endoeffect observed in the DSC curves of $Ba(IO_3)_2 \cdot H_2O$ and $Ba(IO_3)_2 \cdot D_2O$ (Fig. 4(c)) is due to single-stage dehydration.

The isotope effect (T_{max}) in the DSC curves corresponds to that from the DTA curves and shows smaller thermal stability of the deuterate-monohydrates. It must also be pointed out that the values of T_{max} found according to DSC in $M(IO_3)_2 \cdot H_2O$ and in $M(IO_3)_2 \cdot D_2O$ ($M^{2+} = Ca^{2+}$, Sr^{2+}, Ba^{2+}) do not change in the same sequence as in DTA. In $Ba(IO_3)_2 \cdot H_2O$ and $Ba(IO_3)_2 \cdot D_2O$ they are higher than in $Sr(IO_3)_2 \cdot H_2O$ and $Sr(IO_3)_2 \cdot D_2O$ (Tables 1 and 2).

A certain isotope effect may also be observed in relation to $\Delta H^{\ominus}_{deh}$, expressed as $\delta\Delta H^{\ominus}_{deh} = (\delta\Delta H^{\ominus}_{deh})_D - (\delta\Delta H^{\ominus}_{deh})_H$, with the values

For $Ca(IO_3)_2 \cdot H_2O$ (D_2O) $\quad \delta\Delta H^{\ominus}_{deh} = 7.8$ kJ mol^{-1}

For $Sr(IO_3)_2 \cdot H_2O$ (D_2O) $\quad \delta\Delta H^{\ominus}_{deh} = 3.4$ kJ mol^{-1}

For $Ba(IO_3)_2 \cdot H_2O$ (D_2O) $\quad \delta\Delta H^{\ominus}_{deh} = -1.8$ kJ mol^{-1}

The data obtained show that the isotope effect in the compounds examined is not in one direction and differs appreciably in value from one M to another, as established in other compounds [18,19]. In the present case this fact could be explained by the different structures of $Ca(IO_3)_2 \cdot H_2O$ (D_2O) [20], and $Sr(IO_3)_2 \cdot H_2O$ (D_2O) [21] and $Ba(IO_3)_2 \cdot H_2O$ (D_2O) [22]. The last two are isomorphous, but $r_{Sr-O_w} = 253.1$ pm where $r_{Ba-O_w} = 269.5$ pm, which also determines the difference in their $\Delta H^{\ominus}_{deh}$. This difference also affects the isotope effect, although we do not know the extent of the changes of the respective interatomic distances in the deuterates.

TABLE 3

Values of $\Delta H_f^{\ominus}$ for $M(IO_3)_2 \cdot H_2O$ and $M(IO_3)_2 \cdot D_2O$ ($M^{2+} = Ca^{2+}$, Sr^{2+}, Ba^{2+})

Compound	From $\Delta H^{\ominus}_{deh}$ acc. to DSC	Literature		
		Average value	Dispersion S	References
$Ca(IO_3)_2 \cdot H_2O$	1320.4	1310.4	19.8	10, 23, 24
$Ca(IO_3)_2 \cdot D_2O$	1335.1	–	–	–
$Sr(IO_3)_2 \cdot H_2O$	1319.8	1324.7	10.6	10, 23–26
$Sr(IO_3)_2 \cdot D_2O$	1330.65	–	–	–
$Ba(IO_3)_2 \cdot H_2O$	1323.6	1334.1	8.9	10, 23–26
$Ba(IO_3)_2 \cdot D_2O$	1329.2	–	–	–

The values of $\Delta H_f^{\ominus}$ of the ordinary and deuterated monohydrates (Table 3) were calculated on the basis of the value obtained for ΔH_{deh}.

The values of $\Delta H_f^{\ominus}$ calculated for the ordinary hydrates show a fairly high degree of agreement with the data in the literature. No data were found in the literature for the deuterated hydrates. From the calculated $\Delta H_f^{\ominus}$ for the deuterates (other than $Ba(IO_3)_2 \cdot D_2O$) it is possible to calculate also the increment b for the attachment of 1 mol D_2O to the anhydrous salt: the value found is $b = 302.2$ kJ mol^{-1}. This increment also provides for the calculation of $\Delta H_f^{\ominus}$ for other iodate monohydrates.

REFERENCES

1 C. Duval, Anal. Chim. Acta, 20 (1959) 263.
2 Cs. Varhelyi and E. Kekedy, Stud. Univ. Babes-Bolyai, Ser. Chim., 1 (1962) 11.
3 G.E. Ericksen, M.E. Mrose and J.W. Marinenko, J. Res. US Geol. Survey, 2 (1974) 471.
4 Z. Gontarz and A. Gorski, Rocz. Chem., 48 (1974) 2091.
5 Z. Gontarz, A. Gorski and M. Maciejewski, Rocz. Chem., 51 (1977) 1057.
6 M.S. Joshi and S.G. Trivedi, Cryst. Res. Technol., 16 (1981) 19.
7 V.V. Pechkovskii and A.V. Sofronova, Zh. Neorg. Khim., 10 (1965) 1427.
8 H.D. Lutz, H. Klüpel and H. Kesterke, Z. Anorg. Allg. Chem., 423 (1976) 83.
9 P.K. Biswas, A. Roy and K. Nag, Thermochim. Acta, 42 (1980) 91.
10 J. Bousquet and P. Vermande, Bull. Soc. Chim. Fr., 5 (1966) 1552.
11 G.S. Sanyal and K. Nag, J. Inorg. Nucl. Chem., 39 (1977) 1127.
12 E. Alici, Dissertation, Universität Gesamthochschule Siegen, 1990.
13 H.D. Lutz, E. Alici, Th. Kellersohn and P. Kuske, Z. Naturforsch. Teil B, 45 (1990) 587.
14 E. AG. Merck, Komplexometrische Bestimmungsmethoden mit Titriplex, Darmstadt, pp. 21, 41.
15 G. Sharlo, Metodi Analiticheskoi Khimii, Khimiya, Moscow, 1969, p. 1015.
16 M. Maneva and V. Koleva, J. Thermal Anal., in press.
17 I.B. Rabinovich, Vliyanie Izotopii na Fizikokhimicheskie Svoistva Idkostei, Nauka, Moscow, 1968, p. 124.
18 N. Ray Chaudhuri and G.K. Pathak, Thermochim. Acta, 12 (1975) 71.
19 H. Tanaka, Thermochim. Acta, 92 (1985) 215.
20 G.E. Ericksen, M.E. Mrose and J. Marinenko, J. Res. US Geol. Survey, 2 (1974) 471.
21 Am. Manotti Lanfredi, M.A. Pellinghelli, A. Tiripicchio and M. Tiripicchio Camellini, Acta Crystallogr. Sect. B, 28 (1972) 679.
22 H.D. Lutz, E. Alici and W. Buchmeier, Z. Anorg. Allg. Chem., 535 (1985) 31.
23 Handbook of Chemistry and Physics, 61st edn., CRC Press, FL, 1984/1985, p. 66.
24 J. Bousquet, J.C. David, D. Mathurin and G. Perachon, Bull. Soc. Chim. Fr., 10 (1968) 3991.
25 A.A. Shidlovskii and A.A. Voskresenskii, Zh. Fiz. Khim., 40 (1966) 2609.
26 J. Bousquet, D. Mathurin and P. Vermande, Bull. Soc. Chim. Fr., 4 (1969) 1111.